Influence of Spanwise Velocity Distribution on Flow Instability in Inward Swirling Flow

R. Sato[*1] , A. Hiroyama[*1] , M. Kudo[*1] , K. Nishibe[*1] and K. Sato [*2]
[1] Graduate School of Integrative Science and Engineering, Tokyo City University
[2] Department of Mechanical System Engineering, Kogakuin University

* Correspondent author: g2381025@tcu.ac.jp

Abstract

Flow instability with periodic pressure fluctuations are known to occur in the pre-swirling flows generated downstream of inlet guide vanes installed upstream of turbomachinery impellers, and suppression of such flow instability is crucial for realize safe operation. An experimental study was conducted to investigate the effects of different velocity distributions along the channel width on the propagation velocity of the pressure fluctuations and disturbances caused by flow instability. The result show that the asymmetric velocity and flow angle distributions in the vertical direction of the span with respect to its center could reduce the amplitude of the pressure fluctuation caused by the flow instability.

Keyword: *Inlet guide vanes, Swirling flow, Flow instability, Velocity distribution, Pressure fluctuation*

1. Introduction

Inlet guide vanes (IGVs) are mechanical elements installed upstream of the impeller to increase the operating range of the centrifugal compressor and reduce impingement losses by producing a pre-whirling flow. However, below certain flow angles, an inward swirling flow instability is generated downstream of the IGVs. Disturbances called cells with high- and low-pressure regions are generated and observed to propagate in the circumferential direction. These periodic pressure fluctuations cause vibrations in the compressor body and piping system, and there is concern that the piping and components used in the compressor may be damaged due to vibration fatigue. Therefore, there is an urgent need to establish a method for suppressing the flow instability that occurs downstream of IGVs and to clarify the suppression mechanism.

Many studies, both experimental and numerical, have been conducted to elucidate the generation and development mechanism of this disturbance [1–5]. Model experiments have revealed that the effect of blade width on the pressure fluctuation waveform of flow instability with noise is limited, and that the amplitude of pressure fluctuation tends to be larger when the blade string length is longer [1]. The occurrence of flow instability was also confirmed in a linear analysis assuming a two-dimensional inviscid incompressible flow with an infinite number of inlet guide blades, and it was reported that the flow instability is basically a phenomenon of second-order inviscid flow [2–3].

Therefore, our research group has been studying the suppression method of this flow instability focusing on the fact that it is a two-dimensional phenomenon [4–5]. We have proposed a torsional guide blade array in which the guide blade installation angle is continuously varied in the channel width direction and have confirmed that interference with the radial velocity distribution in the test channel width direction is an effective method to break the two-dimensional structure of the disturbance [4]. However, investigations into the influence of the channel-width velocity distribution on the occurrence or non-occurrence of flow instability and vibration characteristics are fragmentary [5], and many unknowns remain.

In this study, we attempted to elucidate the effects of the velocity distribution in the channel width direction on pressure fluctuations and propagation velocity of disturbances due to flow instability by changing the channel width length and adjusting the velocity distribution in the channel width direction. This paper discusses the experimental results when the channel width length b is changed to 10 and 30 mm.

2. Experimental setup

Fig. 1(a) and 1(b) show a schematic of the experimental apparatus and an r-θ cross section of the test channel, respectively. In this study, the same test channels as in previous study [1–2], in which the geometry of the

actual device was simplified, were used. The test channel consisted of 36 IGVs (installation angle β_2 = 20deg, chord length: 10 mm, blade width: 30 mm, and blade thickness: 1 mm) sandwiched between two parallel disc plates (disc radius r_0 = 160 mm). The channel outlet on the lower disk (disk outlet hole radius r_3 = 50 mm) was connected to a plenum tank (530 mm × 530 mm × 800 mm). A blower connected to the plenum tank drew air from the open area into the test channel, and the airflow passed through the IGVs to generate an inward swirling flow downstream of the IGVs. An area flowmeter was used to measure the velocity and flow angle downstream of the IGVs, and a quasi-three-hole pitot tube and pressure transducer were used to measure the velocity, flow angle, and fluctuating pressure, respectively, through each measurement hole on the upper plate (Fig. 1(a)). The number of cells consisting of pairs of high- and low-pressure regions in the disturbance was determined by comparing the angle θ between the two measurement points on the circumference of r_m/r_2 = 0.80 and the phase difference φ calculated from the two measured pressure fluctuation waveforms.

This paper discusses the results obtained under constant values of β_2 = 20deg and r_m/r_2 = 0.4 for the IGVs installation angle β_2, which affects the vibration characteristics and generation limit of the disturbance, and the inner/outer shape ratio r_3/r_2, which is the ratio of the IGV outlet radius to the channel outlet radius, respectively.

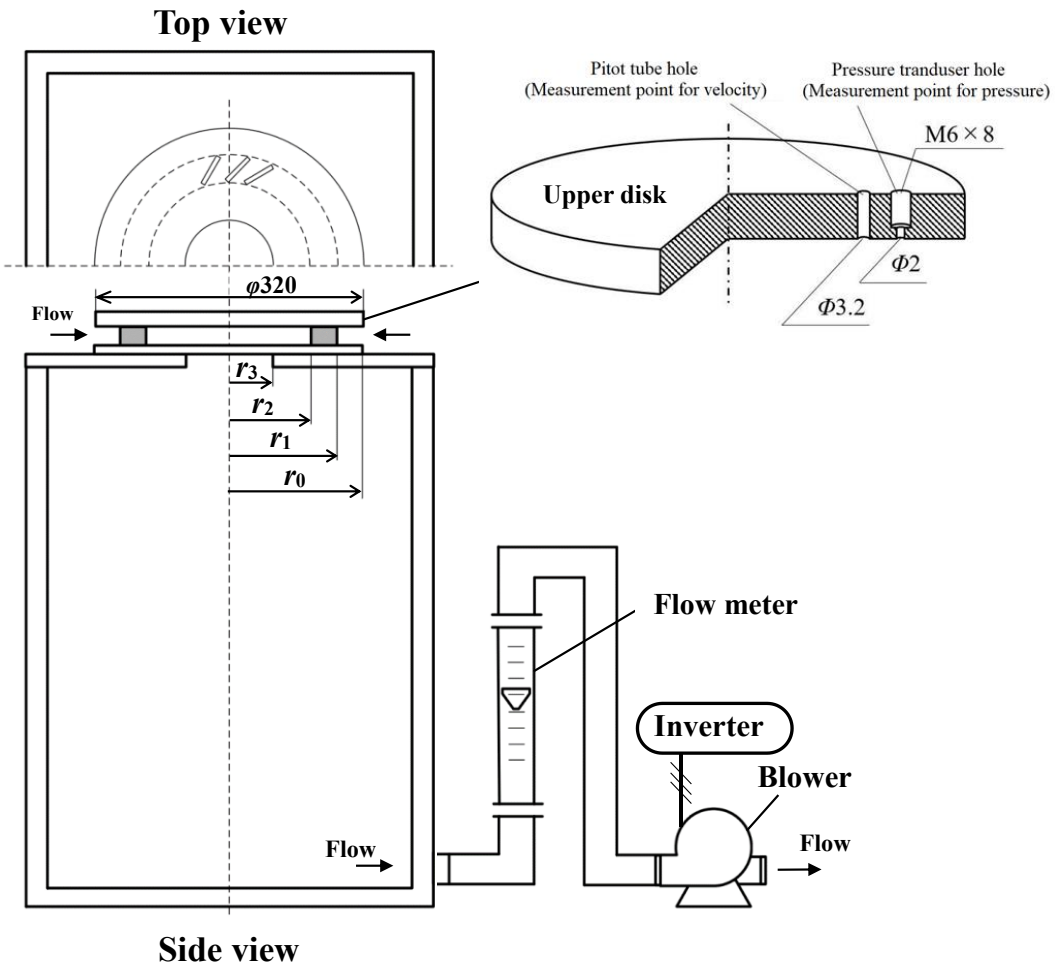

(a) Experimental apparatus

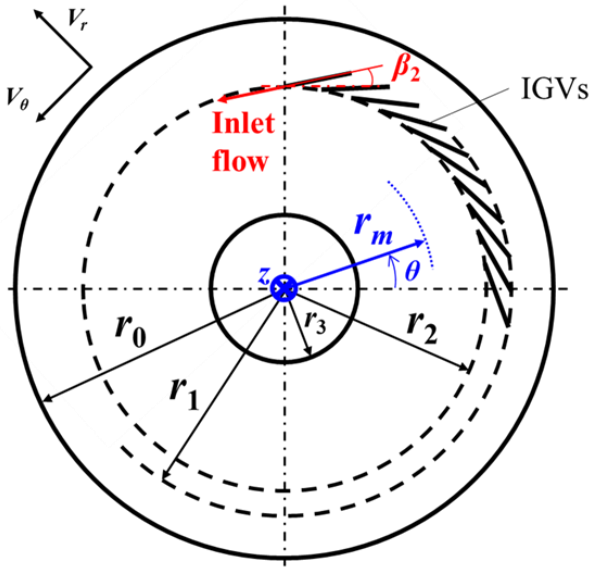

(b) Coordinate system of the test section

Fig. 1 Experimental apparatus and coordinate system

3. Results and discussion

Fig. 2 shows the spanwise distributions of the velocity and flow angle at r_m/r_2 = 0.6, obtained under the constant 2D flow rate Q_{2D} = 0.4 m^2/s. The horizontal axis is b, and the vertical axis velocity distribution is non-dimensionalized by the radial velocity V_{r2} at the IGV outlet. Panels (a) and (b) show for b = 10 and 30 mm, respectively. In both cases, the circumferential velocity V_θ was larger near the center of the channel than that near the channel wall owing to the inward swirling flow, which resulted in the formation of a torsional boundary layer, and the radial velocity V_r near the center of the channel was smaller than that near the wall. Consequently, the flow angle was shallower at the center of the channel than that near the wall. In the case of b = 10 mm, the velocity and flow angle distributions were generally symmetrical in the vertical direction of the span from the midspan, whereas when b = 30 mm, the velocity and flow angle distributions were slightly asymmetrical in the vertical direction of the span. This was probably because the aspect ratio r_2/b, which is the ratio of the IGVs outlet radius r_2 to the span length b, was smaller, and the asymmetry of the test channel outlet geometry had a larger effect.

Figs. 3(a)–(c) show the pressure fluctuation at r_m/r_2 = 0.6 and their frequency analysis and phase difference measurement results, respectively. In addition to the conditions indicated in Figs. 2(a) and 2(b), Q_{2D} = 0.4 m^2/s, the same 3D flow rate as Fig. 2(b) b = 30 mm and Q_{3D} = 1.2 m^2/s (2D flow rate Q_{2D} = 1.2 m^2/s) with b = 10 mm is also shown for reference. The results of the pressure fluctuation waveform, frequency analysis, and phase difference measurements showed that a disturbance with one cell propagated circumferentially under all conditions. As in the previous study, the frequencies of the first dominant component at b = 10 mm (blue solid line) and b = 30 mm (red solid line) under a constant 2D flow rate Q_{2D} = 0.4 m^2/s corresponded approximately at $f \approx$ 11 Hz. For b = 10 mm (green solid line), where the 2D flow rate was tripled, the frequency of the same component was $f \approx$ 33 Hz, which was the same as in the previous study [2], regardless of the span length at this condition range. However, it was confirmed that the pressure fluctuation amplitude when b = 30 mm was approximately 64% smaller than that when b = 10 mm, even under the constant Q_{2D} = 0.4 m^2/s. One possible reason for this is that the two-dimensional nature of the flow instability, which is considered to be essentially a two-dimensional phenomenon [2], was weakened by the spanwise asymmetry of the velocity and flow angle shown in Fig. 2(b) (b = 30 mm), but further investigation is required.

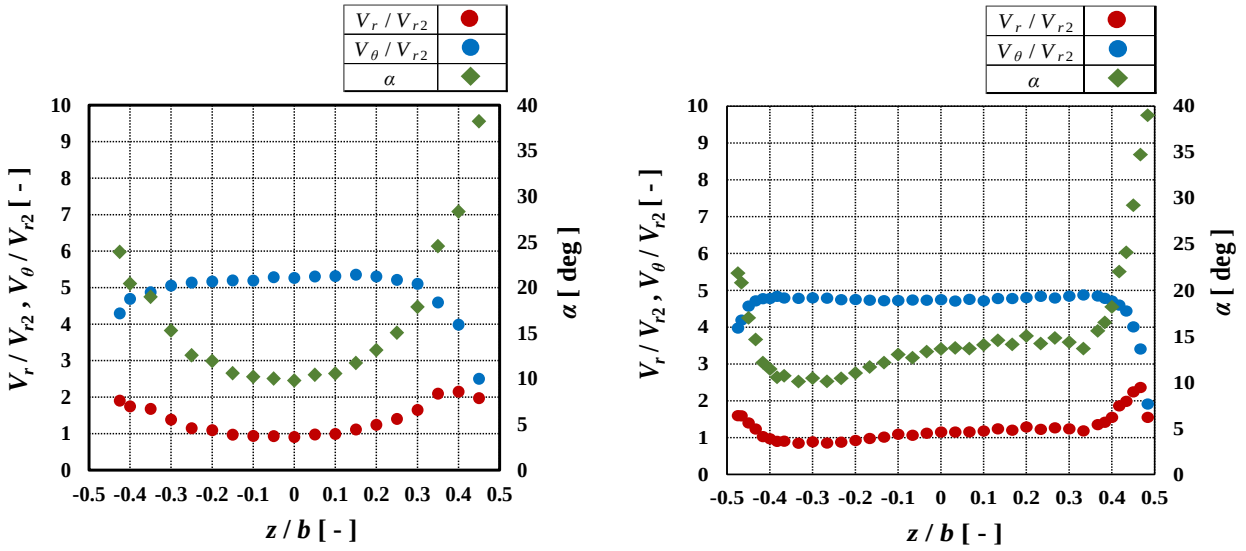

(a) b = 10 mm (b) b = 30 mm

Fig. 2 Spanwise distributions of velocity and flow angle (r_m/r_2 = 0.6, Q = 0.4 m²/s)

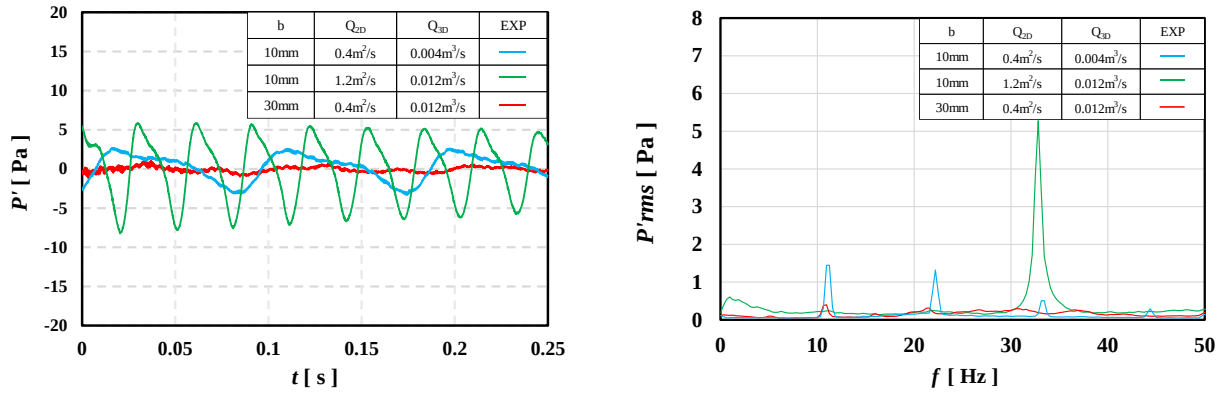

(a) Pressure fluctuations (r_m/r_2 = 0.6) (b)Power spectrums (r_m/r_2 = 0.6)

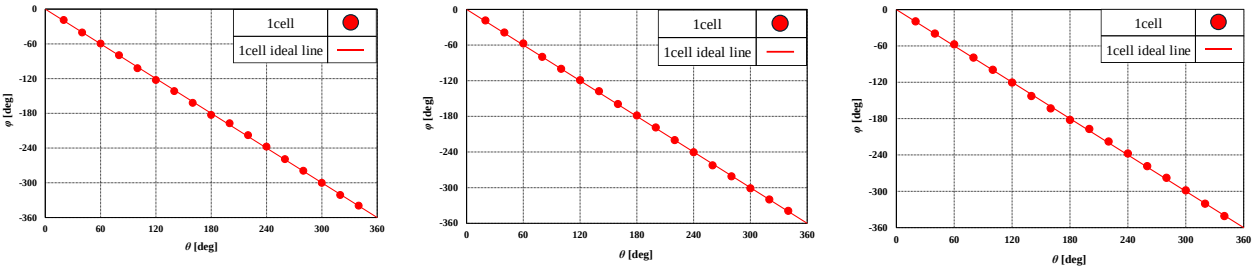

(i) Q = 0.4 m²/s, b = 10 mm (ii) Q = 0.4 m²/s, b = 30 mm (iii) Q = 1.2 m²/s, b = 10 mm

(c) Phase difference (r_m/r_2 = 0.8)

Fig. 3 Pressure fluctuation waveforms, frequency, and phase difference

4. Conclusions

In this study, we experimentally investigated the effects of the velocity distribution along the channel width and flow angle on the fluctuating pressure and propagation velocity of disturbances in the flow instability generated downstream of IGVs, primarily under the same two-dimensional flow rate conditions. The results showed that asymmetric flow angles and velocity profiles in the spanwise direction may suppress the amplitude

of pressure fluctuations. However, systematic verification with larger asymmetries is required to confirm the effect of the asymmetry.

Nomenclature

A	:	Pressure fluctuation amplitude [Pa]
b	:	Width of test flow channel [mm]
f	:	Frequency [Hz]
P'	:	Pressure fluctuation [Pa]
P'_{rms}	:	Pressure fluctuation RMS [Pa]
Q_{2D}	:	Two-dimensional flow rate [m^2 /s]
Q_{3D}	:	Three-dimensional flow rate [m^3 /s]
r	:	Radius [mm]
t	:	Time [s]
V	:	Velocity [m/s]
V_r	:	Radial velocity [m/s]
V_θ	:	Circumferential velocity [m/s]
z	:	Coordinate axes in the direction of channel width [-]
α	:	Flow angle [deg]
β	:	Installation angle of guide vanes [deg]
θ	:	Angle between measurement points of pressure fluctuation [deg]
φ	:	Phase difference of pressure fluctuation waveform [deg]

Subscript

0	:	Inlet of the device
1	:	Leading edge of the vanes
2	:	Trailing edge of the vanes
3	:	Outlet of the device
m	:	Measurement point

References

[1] Takama N., and Yoshiki H., "Unstable Flow Around Rear Part of Inlet Guide Vanes. Effect of Guide Vane Chord Length," *Proceedings of the 12th Autumn Conference of Gas Turbine Society of Japan*, pp. 33-38, 1997.

[2] Sato K., Nagao K., Tsujimoto Y., Cho K. and Yoshiki H., "Study of Flow Instabilities Downstream of Radial Inlet Guide Vanes," *Trans. JSME*, Vol. 66, No. 646, pp. 141-148, 2000. DOI:10.1299/kikaib.66.646_1399

[3] Nishibe K., Sato K., Tsujimoto Y., and Yoshiki H. (2011). Control of flow instabilities downstream of radial inlet guide vanes. Journal of Fluid Science and Technology, 6(4), 651-661.

[4] Noda K. et al. (2017): "Investigation of Flow Instabilities in Inward Swirling Flow in Rotating Machinery". Conference of ICJWSF-2017, 38, pp. 1-6

[5] Ichikawa K., Kudo M., Sato R., Nishibe K., and Sato K. "Influence of Span Length on Flow Instability Downstream of Inlet Guide Vanes," Proceedings of the 9th World Congress on Mechanical, Chemical, and Material Engineering, 2023, DOI: 10.11159/htff23.185